Available online at www.sciencedirect.com

ScienceDirect

Polyhedron 27 (2008) 411–419

POLYHEDRON

www.elsevier.com/locate/poly

# Novel octahedral nickel(II) dithiocarbamates with bi- or tetradentate *N*-donor ligands: X-ray structures of [Ni(Bzppzdtc)(phen)$_2$]ClO$_4$ · CHCl$_3$ and [Ni(Bz$_2$dtc)$_2$(cyclam)]

Zdeněk Trávníček [a,*], Richard Pastorek [a], Václav Slovák [b]

[a] *Department of Inorganic Chemistry, Faculty of Science, Palacký University, Křížkovského 10, CZ-771 47 Olomouc, Czech Republic*
[b] *Department of Chemistry, Faculty of Science, University of Ostrava, 30. dubna 22, CZ-701 03 Ostrava, Czech Republic*

Received 12 July 2007; accepted 28 September 2007
Available online 5 November 2007

---

**Abstract**

A series of novel octahedral nickel(II) dithiocarbamate complexes involving bidentate nitrogen-donor ligands (phen = 1, 10-phenanthroline, bpy = 2,2′-bipyridine) or a tetradentate ligand (cyclam = 1,4,8,11-tetraazacycloteradecane) of the composition [Ni(BzMetdtc)(phen)$_2$]ClO$_4$ (**1**), [Ni(Pe$_2$dtc)(phen)$_2$]ClO$_4$ (**2**), [Ni(Bzppzdtc)(phen)$_2$]ClO$_4$ · CHCl$_3$ (**3**), [Ni(Bzppzdtc)(phen)$_2$](SCN) (**4**), [Ni(BzMetdtc)(bpy)$_2$]ClO$_4$ · 2H$_2$O (**5**), [Ni(Pe$_2$dtc)(cyclam)]ClO$_4$ (**6**), [Ni(BzMetdtc)$_2$(cyclam)] (**7**), [Ni(Bz$_2$dtc)$_2$(cyclam)] (**8**) and [Ni(Bz$_2$dtc)$_2$(phen)] (**9**) (BzMetdtc = *N*,*N*-benzyl-methyldithiocarbamate(1-) anion, Pe$_2$dtc = *N*,*N*-dipentyldithiocarbamate(1-) anion, Bz$_2$dtc = *N*,*N*-dibenzyldithiocarbamate(1-) anion, Bzppzdtc = 4-benzylpiperazinedithiocarbamate(1-) anion), have been synthesized. Spectroscopic (electronic and infrared), magnetic moment and molar conductivity data, and thermal behaviour of the complexes are discussed. Single crystal X-ray analysis of **3** and **8** confirmed a distorted octahedral arrangement in the vicinity of the nickel atom with a N$_4$S$_2$ donor set. They represent the first X-ray structures of such type complexes. The catalytic influence of complexes **2**, **3**, **6**, and **7** on graphite oxidation was studied and discussed.

*Keywords:* Nickel(II); Dithiocarbamates; X-ray structures; Graphite oxidation

---

## 1. Introduction

Generally, it is well known that square-planar dithiocarbamates (dtc) of nickel(II) of the type [Ni(dtc)$_2$] react very unreadily with nitrogen-donor ligands. To date, only a few data regarding this topic have been found in the literature. For instance, Coucouvanis and Fackler [1] studied reactions of the mentioned Ni(II)-dithiocarbamates with monodentate N-donor ligands and synthesized paramagnetic octahedral complexes [Ni(H$_2$dtc)$_2$($\gamma$-pic)$_2$], [Ni(H$_2$dtc)$_2$(py)$_2$] and [Ni(HRdtc)$_2$($\gamma$-pic)$_2$] (R = chlorophenyl; $\gamma$-pic = $\gamma$-picoline, py = pyridine). Moreover, the authors also found that [Ni(Et$_2$dtc)$_2$] (Et = ethyl) forms adducts with pyridine and $\gamma$-picoline at liquid nitrogen temperature. The same conclusion was also confirmed by Dingle [2]. On the contrary, Ramalingam and co-workers [3] were unsuccessful in the preparation of pyridine and ethylenediamine (en) adducts of [Ni(Et$_2$dtc)$_2$], [Ni(HEadtc)$_2$] and [Ni(Ea$_2$dtc)$_2$] (H$_2$Eadtc = ethanoldithiocarbamic acid). They had only found that in the case of attempts to prepare the discussed adducts with ethylenediamine, the reactions led to the formation of $[Ni(en)_3]^{2+}[(dtc)_2]^{2-}$ and/or [Ni(en)$_3$]S$_2$O$_3$, respectively.

Formerly, as a continuation in our systematic study of dithiocarbamate transition metal complexes, especially of nickel, we have prepared and characterized a binuclear complex {[Ni(Ea$_2$dtc)$_2$]$_2$($\mu$-en)} in which two nickel(II) ions

---

[*] Corresponding author. Tel.: +420 58 5634350; fax: +420 58 5634352.
*E-mail address:* zdenek.travnicek@upol.cz (Z. Trávníček).

0277-5387/$ - see front matter © 2007 Elsevier Ltd. All rights reserved.
doi:10.1016/j.poly.2007.09.024

are connected via an ethylenediamine bridge [4]. We have also synthesized octahedral [Ni(Bz$^i$Prdtc)$_2$(cyclam)] and [Ni(Bz$^i$Prdtc)(cyclam)]X complexes, where cyclam = 1,4,8,11-tetraazacyclodecane, Bz$^i$Prdtc = *N*,*N*-benzylisopropyldithiocarbamate, (X = ClO$_4$, BPh$_4$) [5]. Moreover, the [Ni(Bz$^i$Prdtc)(cyclam)]BPh$_4$ · CHCl$_3$ complex has been structurally characterized by single crystal X-ray analysis. In search for X-ray structures deposited within the Cambridge Structural Database [6] involving any transition metal in combination with a dithiocarbamate moiety and any N-donor ligand, and bearing a N$_4$S$_2$ donor set, ten molecular structures complying with the above-mentioned requirement have been found, i.e. four mononuclear Ru(II) complexes [7–9], three dinuclear Mo(V) complexes [10–12], two mononuclear Co(III) [13,14] complexes, and one mononuclear Ni(II) complex [15].

In this paper, we report the synthesis and characterization of novel octahedral Ni(II)-dithiocarbamate complexes **1**–**9** along with the single crystal X-ray structures of **3** and **8**. Moreover, the methods of thermal analysis have been used for the study of influence of selected complexes on graphite oxidation. This possible practical utilization of Ni(II)-dithiocarbamates have been also described and discussed recently in case of similar complexes [16,17].

## 2. Experimental

### 2.1. Materials

Dipentylamine (97%), 1-benzylpiperazine (98%), 1,4,8,11-tetraazacyclodecane (cyclam), nitromethane and K[PF$_6$] were supplied by FLUKA Co. 1,10-Phenanthroline (phen), 2,2′-bipyridine (bpy), LiClO$_4$ · 3H$_2$O and dibenzylamine (97%) were acquired from SIGMA ALDRICH Co. and *N*-benzylamine (97%) from LANCASTER Co. The remaining reagents were obtained from LACHEMA Co., all of p.a. purity.

### 2.2. Syntheses

#### 2.2.1. [Ni(BzMetdtc)$_2$]

The complex was prepared by a slightly modified procedure described previously [18]. *N*-Benzylmethylamine (64 mL, 50 mmol) was added drop-wise into a solution of CS$_2$ (3 mL, 50 mmol) in ethanol (96%, 25 mL) with stirring. The reaction mixture was left to stand at room temperature for a short time period. Then, a warm solution of NiCl$_2$ · 6H$_2$O (5.9 g, 25 mmol) in distilled water (50 mL) was added. After the solution addition, the light green precipitate of [Ni(BzMetdtc)$_2$] appeared. It was filtered off, washed with warm water (until negative reaction on Cl$^-$ ions) and dried at 40 °C under an infrared lamp. Yield: 72%. *Anal.* Calc. for $C_{18}H_{20}N_2NiS_4$: C, 47.9; H, 4.5; N, 6.2; Ni, 13.0; S, 28.4. Found: C, 48.0; H, 4.4; N, 5.9; Ni, 12.8; S, 28.7%.

#### 2.2.2. [Ni(BzMetdtc)(phen)$_2$]ClO$_4$ (1) and [Ni(BzMetdtc)(bpy)$_2$]ClO$_4$ · 2H$_2$O (5)

To a suspension of finely powdered [Ni(BzMetdtc)$_2$] (0.23 g, 0.5 mmol) in an ethanol/chloroform mixture (30/30 mL), NiCl$_2$ · 6H$_2$O (0.11 g, 0.5 mmol), LiClO$_4$ · 3H$_2$O (0.16 g, 1 mmol) and bpy (0.31 g, 2 mmol) or phen (0.39 g, 2 mmol) were added in this sequence. The reaction mixture was stirred under reflux for 20 h and then filtered. The solid formed after 5 days. It was filtered off, washed with ethanol and diethyl ether, and recrystallized from a chloroform solution with activated carbon. The substance which formed, was filtered off, washed with diethyl ether and dried under an infrared lamp at 40 °C. Yields: 56% (**1**) and 73% (**5**). *Anal.* Calc. for $C_{33}H_{26}N_5NiS_2ClO_4$ (**1**): C, 55.4; H, 3.7; N, 9.8; Ni, 8.2; S, 9.0; Cl, 5.0. Found: C, 54.9; H, 3.4; N, 9.5; Ni, 8.3; S, 8.8; Cl, 4.8%. *Anal.* Calc. for $C_{29}H_{30}N_5NiS_2ClO_6$ (**5**): C, 49.6; H, 4.3; N, 10.0; Ni, 8.3; S, 9.1; Cl, 5.0. Found: C, 49.8; H, 4.2; N, 10.2; Ni, 8.2; S, 8.9; Cl, 4.7%.

#### 2.2.3. [Ni(Pe$_2$dtc)(phen)$_2$]ClO$_4$ (2)

Phen (0.40 g, 2 mmol) and LiClO$_4$ · 3H$_2$O (0.16 g, 1 mmol) were added in this sequence to a suspension of finely powdered [Ni(Pe$_2$dtc)$_2$] [8] (0.52 g, 1 mmol) in methanol (15 mL). The reaction mixture was stirred under reflux until the colour of the solution turned to red (2 h). Then, the solution was filtered with activated carbon and the filtrate was left to stand at room temperature. After several hours, crystals formed in the mother liquor from which single crystals suitable for X-ray analysis were selected. The remaining portion of the crystalline product was filtered off, washed with methanol and diethyl ether and dried under an infrared lamp at 40 °C. Yield: 81%. *Anal.* Calc. for $C_{35}H_{38}N_5NiS_2ClO_4$ (**2**): C, 56.0; H, 5.1; N, 9.3; Ni, 7.8; S, 8.5; Cl, 4.7. Found: C, 56.1; H, 5.0; N, 9.3; Ni, 8.0; S, 8.3; Cl, 4.8%.

#### 2.2.4. [Ni(Bzppzdtc)$_2$]

The complex was prepared by a slightly modified procedure described previously [18]. 1-Benzylpiperazine (8.7 mL, 50 mmol) was added drop-wise to a solution of CS$_2$ (3 mL, 50 mmol) in ethanol (96%, 25 mL) with stirring. A white precipitate, which formed during the above reaction, was dissolved by adding a solution of NaOH (1.9 g, 50 mmol) in water (10 mL). The resulting solution was filtered and a warm solution of NiCl$_2$ · 6H$_2$O (5.9 g, 25 mmol) in water (50 mL) was added with stirring to the filtrate. Subsequent steps are identical to those described for the preparation of [Ni(BzMetdtc)$_2$] (see Section 2.2.1). Yield: 81%. *Anal.* Calc. for $C_{24}H_{30}N_4NiS_4$: C, 51.3; H, 5.4; N, 10.0; Ni, 10.5; S, 22.8. Found: C, 51.0; H, 5.1; N, 9.8; Ni, 10.6; S, 22.5%.

#### 2.2.5. [Ni(Bzppzdtc)(phen)$_2$]ClO$_4$ · CHCl$_3$ (3)

A mixture of finely powdered [Ni(Bzppzdtc)$_2$] (0.39 g, 2 mmol), phen (0.39 g, 2 mmol), NiCl$_2$ · 6H$_2$O (0.11 g, 0.5 mmol) and LiClO$_4$ · 3H$_2$O (0.16 g, 1 mmol) were suspended in an ethanol/chloroform mixture (15/15 mL).

The reaction mixture was stirred under reflux until all components dissolved and the colour of the solution turned to dark red (*ca.* 4 h). Then, the solution was filtered with activated carbon and the filtrate was left to stand at room temperature for 7 days. During this period, a green substance appeared and it was separated by filtration and discarded. Subsequently, brown crystals suitable for X-ray analysis formed in the mother liquor after several days. They were filtered off, washed with hexane and dried under an infrared lamp at 40 °C. Yield: 56%. *Anal.* Calc. for $C_{37}H_{32}N_6NiS_2Cl_4O_4$ (**3**): C, 50.0; H, 3.6; N, 9.4; Ni, 6.6; S, 7.2; Cl, 15.9. Found: C, 50.4; H, 3.3; N, 9.5; Ni, 6.3; S, 7.0; Cl, 15.6%.

### 2.2.6. *[Ni(Bzppzdtc)(phen)$_2$](SCN) (**4**)*

Finely powdered [Ni(Bzppzdtc)$_2$] (0.28 g, 0.5 mmol) together with phen (0.39 g, 2 mmol) and $Ni(SCN)_2 \cdot 2H_2O$ (0.11 g, 0.5 mmol) were suspended in an ethanol/chloroform mixture (15/15 mL) and stirred under reflux for 4 h. After filtration of the reaction mixture with activated carbon, a light brown precipitate formed in the mother liquor in the course of a few days. The product was filtered off, washed with hexane and dried under an infrared lamp at 40 °C. Yield: 57%. *Anal.* Calc. for $C_{37}H_{31}N_7NiS_3$ (**4**): C, 61.0; H, 4.3; N, 13.5; Ni, 8.1; S, 13.2. Found: C, 60.4; H, 4.2; N, 13.2; Ni, 7.9; S, 13.5%.

### 2.2.7. *[Ni(Pe$_2$dtc)(cyclam)]ClO$_4$ (**6**)*

A suspension of finely powdered [Ni(Pe$_2$dtc)$_2$] (0.52 g, 1 mmol) in chloroform (5 mL) was mixed while stirring with 1,4,8,11-tetraazacyclodecane (0.2 g, 1 mmol) in 96% ethanol (5 mL) and $LiClO_4 \cdot 3H_2O$ (0.16 g, 1 mmol) in 96% ethanol (3 mL). The reaction mixture was stirred under reflux for 10 h. The resulting violet solution was filtered with activated carbon and left to stand at room temperature. After one week, a viscous product was obtained which was extracted with diethyl ether. After three days, the viscous product was formed again from which a powdered substance was isolated by means of diethyl ether. It was filtered off and dried under an infrared lamp at 40 °C. Yield: 46%. *Anal.* Calc. for $C_{21}H_{46}N_5NiS_2ClO_4$ (**6**): C, 42.7; H, 7.8; N, 11.8; Ni, 9.9; S, 10.8; Cl, 6.0. Found: C, 42.5; H, 7.5; N, 11.6; Ni, 9.8; S, 10.5; Cl, 5.5%.

### 2.2.8. *[Ni(BzMetdtc)$_2$(cyclam)] (7) and [Ni(Bz$_2$dtc)$_2$(cyclam)] (**8**)*

These compounds were obtained by the reaction of finely powdered [Ni(Bz$_2$dtc)$_2$] (0.6 g, 1 mmol) or [Ni(BzMetdtc)$_2$] (0.45 g, 1 mmol) in chloroform (5 mL) with 1,4,8,11-tetraazacyclodecane (cyclam) (0.2 g, 1 mmol) in 96% ethanol (10 mL). The mixture was stirred under reflux for 10 h and the resulting violet solution was filtered. During a few days, violet crystals, or a violet powder substance appeared. The product was recrystallized from chloroform by addition of methanol or hexane. The violet powder substance and violet crystals were isolated in the case of (**7**), and (**8**), respectively, which were washed with methanol or hexane and dried under an infrared lamp at 40 °C. Yields: 62% (**7**) and 58% (**8**). *Anal.* Calc. for $C_{28}H_{44}N_4NiS_4$ (**7**): C, 51.6; H, 6.8; N, 12.9; Ni, 9.0; S, 19.7. Found: C, 51.1; H, 7.2; N, 12.8; Ni, 8.9; S, 19.5%. *Anal.* Calc. for $C_{40}H_{52}N_6NiS_4$ (**8**): C, 59.8; H, 6.5; N, 10.4; Ni, 7.3; S, 16.0. Found: C, 59.3; H, 6.9; N, 10.5; Ni, 7.8; S, 15.7%.

### 2.2.9. *[Ni(Bz$_2$dtc)$_2$(phen)] (**9**)*

Phen (0.20 g, 1 mmol) and $LiClO_4 \cdot 3H_2O$ (0.16 g, 1 mmol) were added to a suspension of finely powdered [Ni(Bz$_2$dtc)$_2$] (0.60 g, 1 mmol) in methanol (15 mL) with stirring and the mixture was refluxed for 30 min. Then, a yellow substance formed. It was filtered off, washed with methanol, and dried under an infrared lamp at 40 °C. Yield: 85%. *Anal.* Calc. for $C_{42}H_{36}N_4NiS_4$ (**9**): C, 64.4; H, 4.6; N, 7.1; Ni, 7.5; S, 16.4. Found: C, 64.1; H, 4.2; N, 7.4; Ni, 7.3; S, 16.1%.

## 2.3. *Physical measurements*

The nickel content was determined by chelatometric titration using murexide as an indicator [19]. Chlorine content was determined by the Schöniger method [20]. CHNS analyses were performed on an EA 1108 analyzer (Fisons Instruments) instrument with satisfactory results for all the prepared complexes. Room temperature magnetic susceptibilities were measured by Faraday method on a laboratory designed instrument equipped with a Sartorius 4434 MP-8 microbalance, using Co[Hg(NCS)$_4$] as a calibrant. The correction for diamagnetism was performed using Pascal constants. Conductivities were measured with an LF 330/SET conductivity meter (WTW GmbH) at 25 °C. Diffuse-reflectance (45 000–9090 $cm^{-1}$) and DMFA solution (30 000–9090 $cm^{-1}$) electronic spectra were carried out on a Perkin–Elmer Lambda35 UV/Vis spectrometer. Nujol technique. IR spectra (4000–450 $cm^{-1}$) were recorded on a Perkin–Elmer Spectrum One FT-IR spectrometer using the KBr technique. TG/DTA analyses were performed on an Exstar TG/DTA 6200 (Seiko Instruments, Inc.) with the heating rate of 2.5 °C $min^{-1}$, sample weight of 7–11 mg, and temperature range of 20–1050 °C.

The study the catalytic influence of the complexes **2**, **3**, **6**, and **7** on graphite was performed on a Netzsch STA 449C device with an $\alpha$-$Al_2O_3$ crucible without a standard, heating rate of 10 °C $min^{-1}$, a sample weight of 4.4–5.1 mg, and in a dynamic atmosphere (air, 100 $cm^3$ $min^{-1}$). Samples for the study were prepared by the mixing of graphite (0.6 g, diameter of particles less than 0.1 mm, ash residue max. 0.2%, mass drying loss max. 0.2%) with an acetone solution (2 mL) of the appropriate complex (**2**, **3**, **6** and **7**; [Ni] = 2.5 mM). All samples were homogenized by means of stirring and drying at room temperature for 24 h. Each experimental result is represented as an arithmetic mean of three independent experiments. The kinetic parameters were calculated by a direct non-linear regression method [21].

Table 1
Crystal data and structure refinement for [Ni(Bzppzdtc)(phen)$_2$]ClO$_4$ · CHCl$_3$ (**3**) and [Ni(Bz$_2$dtc)$_2$(cyclam)] (**8**)

| | **3** | **8** |
|---|---|---|
| Empirical formula | $C_{37}H_{32}Cl_4N_6NiO_4S_2$ | $C_{40}H_{46}N_6NiS_4$ |
| Formula weight | 889.32 | 797.78 |
| Temperature (K) | 105(2) | 105(2) |
| Wavelength (Å) | 0.71073 | 0.71073 |
| Crystal system, space group | $P2_1/c$ | $P2_1/c$ |
| $a$ (Å) | 12.799(3) | 9.2729(3) |
| $b$ (Å) | 16.864(3) | 19.7667(5) |
| $c$ (Å) | 17.691(5) | 10.8490(4) |
| $\alpha$ (°) | 90 | 90 |
| $\beta$ (°) | 92.18(2) | 97.151(3) |
| $\gamma$ (°) | 90 | 90 |
| Volume (Å$^3$) | 3815.7(17) | 1973.09(117) |
| $Z$, calculated density (g cm$^{-3}$) | 4, 1.548 | 2, 1.343 |
| Absorption coefficient (mm$^{-1}$) | 0.948 | 0.740 |
| $F(000)$ | 1824 | 840 |
| Crystal size | 0.40 × 0.35 × 0.30 mm | 0.40 × 0.40 × 0.30 mm |
| $\theta$ range for data collection (°) | 2.68–25.00 | 2.80–25.00 |
| Index ranges | $-15 \leqslant h \leqslant 15$, $-20 \leqslant k \leqslant 20$, $-15 \leqslant l \leqslant 21$ | $-11 \leqslant h \leqslant 10$, $-23 \leqslant k \leqslant 13$, $-12 \leqslant l \leqslant 12$ |
| Reflections collected/unique | 33494/6713 ($R_{int} = 0.0282$) | 10042/3462 ($R_{int} = 0.0201$) |
| Refinement method on $F^2$ | full-matrix least-squares | full-matrix least-squares |
| Goodness-of-fit on $F^2$ | 0.983 | 1.020 |
| Final $R$ indices [$I > 2\sigma(I)$] | $R_1 = 0.0424$, $wR_2 = 0.1197$ | $R_1 = 0.0594$, $wR_2 = 0.1265$ |
| $R$ indices (all data) | $R_1 = 0.0562$, $wR_2 = 0.1289$ | $R_1 = 0.0762$, $wR_2 = 0.1329$ |
| Largest difference in peak and hole (e Å$^{-3}$) | 0.727 and −0.979 | 0.820 and −0.552 |

### 2.4. X-ray structures

X-ray data collections for **3** and **8** were performed on an Oxford Diffraction Xcalibur™2 equipped with a Sapphire2 CCD detector using Mo K$\alpha$ radiation at 105 K. The CRYSALIS program package (version 1.171.32.5, Oxford Diffraction) was used for data collection and reduction. The molecular structure of **3** was solved by direct methods [SHELXS-97] [22] and all non-hydrogen atoms were refined anisotropically on $F^2$ using full-matrix least-squares procedure [SHELXL-97] [23] with weight: $w = 1/[\sigma^2(F_o)^2 + (0.08P)^2 + 5.00P]$, where $P = (F_o{}^2 + 2F_c{}^2)/3$. All H-atoms of **3** were found in differential maps of electron density and their parameters were refined using the riding model with the C–H distance of 0.95, 0.99, and 1.00 Å, respectively, and with $U_{iso}(H) = 1.2U_{eq}(C)$. Additional calculations were performed using the DIAMOND program [24]. The molecular structure of **8** was solved by direct methods [SHELXS-97] and all non-hydrogen atoms were refined anisotropically on $F^2$ using full-matrix least-squares procedure [SHELXL-97] with weight: $w = 1/[\sigma^2(F_o)^2 + (0.03P)^2 + 5.00P]$. The structure of **8** consists of a centrosymmetric Ni$_{1/2}$(Bz$_2$dtc)(cyclam)$_{1/2}$ moiety which is connected with its second part by means of an inversion centre [symmetry code: $^a$ $-x, -y+1, -z+1$] lying in the middle of Ni1···Ni1a distance. The separation of Ni1···Ni1a is 2.3962(16) Å. The N2–N4 and C20 atoms of the moiety belonging to cyclam are disordered over two positions with the occupancy of 36% (for N2 and N4), 64% (for N3), 32% (for C20) and 33% (for C20b), and 14% (for N2a and N4a), 36% (for N3a), 15% (for C20a) and 20% (for C20c). Owing to the high degree of disorder, a relatively high number of restrains (≈91) have been applied during the structural refinement of **8**, and moreover, a few H-atoms were not included into the refinement. H-atoms were positioned theoretically and refined using the riding model with the C–H distances of 0.95 and 0.99 Å, and N–H distance of 0.93 Å. Crystal data and structure refinements for both the structures are given in Table 1.

## 3. Results and discussion

### 3.1. General characterization

Colours, magnetic moment, molar conductivity and spectral data of all the prepared complexes **1**–**9** are summarized in Table 2. All complexes are paramagnetic with values of effective magnetic moments ranging from 3.02 to 3.41$\mu_{eff}/\mu_B$. These values indicate the presence of two unpaired electrons and show on octahedral geometry in the vicinity of the nickel atom [25]. The octahedral geometry can also be supported by the d–d transition bands revealed both in electronic diffuse-reflectance and DMFA solution spectra at 10280–11720, 16180–19960 and 21929–26230 cm$^{-1}$ (see Table 3). They may be assigned to the $^3A_{2g} \rightarrow {}^3T_{2g}$ ($\nu_1$), $^3A_{2g} \rightarrow {}^3T_{1g}$ ($F$) ($\nu_2$), and $^3A_{2g} \rightarrow {}^3T_{1g}(P)$ ($\nu_3$) transitions, respectively [26]. The maxima above 30000 cm$^{-1}$ are probably caused by charge-transfer transitions. An ionic nature of complexes **1**–**6** may be supported by their molar conductivity data. It has been found that the complexes behave as 1:1 electrolytes in acetone or DMFA solution [27]. Their molar conductivity values are

Table 2
Colour, molar conductivity, magnetic moment, spectral and thermal data for the complexes

| | Colour | $\lambda_M$ (S cm$^2$ mol$^{-1}$) | $\mu_{eff}/\mu_B$ | IR (cm$^{-1}$) | | | TA[a] (°C) |
|---|---|---|---|---|---|---|---|
| | | | | $\nu$ (C—S) | $\nu$ (C—N) | | |
| **1** | yellow | 148.6[b] | 3.04 | 994m | 1515w | $\nu_3(ClO_4^-)$: 1089vs; $\nu_4(ClO_4^-)$: 623s | [c] |
| **2** | dark red | 146.2[b] | 3.21 | 992m | 1515s | $\nu_3(ClO_4^-)$: 1096vs; $\nu_4(ClO_4^-)$: 623vs | [c] |
| **3** | dark brown | 132.8[b] | 3.16 | 996m | 1514m | $\nu_3(ClO_4^-)$: 1095vs; $\nu_4(ClO_4^-)$: 622s | [c] |
| **4** | light brown | 147.2[d] | 3.41 | 996s | 1515vs | $\nu_{as}(C{\equiv}N)$: 2083vs | 193 |
| **5** | yellow | 135.5[b] | 3.02 | 992m | 1514m | $\nu_3(ClO_4^-)$: 1084m; $\nu_4(ClO_4^-)$: 626m | [c] |
| **6** | light violet | 111.1[b] | 3.07 | 995m | 1493s | $\nu_3(ClO_4^-)$: 1087vs; $\nu_4(ClO_4^-)$: 624vs | [c] |
| **7** | light violet | 3.4[b] | 3.07 | 996m | 1522m | | 134 |
| **8** | violet | 25.2[d] | 3.12 | 983vs | 1493s | | 163 |
| **9** | grey | 10.0[d] | 3.20 | 999vs | 1513m | | 190 |

(**1**) [Ni(BzMetdtc)(phen)$_2$]ClO$_4$; (**2**) [Ni(Pe$_2$dtc)(phen)$_2$]ClO$_4$; (**3**) [Ni(Bzppzdtc)(phen)$_2$]ClO$_4$ · CHCl$_3$; (**4**) [Ni(Bzppzdtc)(phen)$_2$](SCN); (**5**) [Ni(BzMetdtc)(bpy)$_2$]ClO$_4$ · 2H$_2$O; (**6**) [Ni(Pe$_2$dtc)(cyclam)]ClO$_4$; (**7**) [Ni(BzMetdtc)$_2$(cyclam)]; (**8**) [Ni(Bz$_2$dtc)$_2$(cyclam)]; (**9**) [Ni(Bz$_2$dtc)$_2$(phen)].

[a] The beginning of thermal decomposition.

[b] Measured in acetone.

[c] Did not studied owing to the explosiveness.

[d] Measured in DMFA solution.

Table 3
UV/Vis spectral data for the complexes

| | Diffuse-reflectance | UV/Vis[a] Solution[b] | ε (dm$^3$ cm$^{-1}$ mol$^{-1}$) |
|---|---|---|---|
| **1** | 11720 | 10834 | 14 |
| | 26230 | 11363 | 27 |
| | 31100 | 17391 | 87 |
| | | 25125 | 675 |
| **2** | 11810 | 10294 | 14 |
| | 19620 | 11194 | 28 |
| | | 19792 | 17 |
| | | 25252 | 512 |
| **3** | 11540 | 10718 | 17 |
| | 19810 | 11376 | 24 |
| | | 19960 | 131 |
| | | 25316 | 532 |
| **4** | 10680 | 10256 | 8 |
| | 17790 | 11641 | 10 |
| | | 16181 | 31 |
| | | 20040 | 96 |
| **5** | 11690 | 10638 | 12 |
| | 167·80 | 16393 | 36 |
| | 24050 | 20000 | 96 |
| | 30030 | 24398 | 156 |
| **6** | 11240 | 10752 | 47 |
| | 17790 | 11350 | 55 |
| | 31480 | 17921 | 73 |
| | | 23201 | 75 |
| **7** | 10530 | 10791 | 35 |
| | 16180 | 11287 | 44 |
| | 22440 | 18116 | 67 |
| | 30100 | 22676 | 77 |
| **8** | 11320 | 10799 | 16 |
| | 18110 | 11363 | 17 |
| | | 18018 | 28 |
| | | 24937 | 72 |
| **9** | 10280 | 10706 | 15 |
| | 16280 | 11389 | 24 |
| | 20390 | 20040 | 80 |
| | | 21929 | 86 |

[a] Absorption maxima in cm$^{-1}$.

[b] Measured in DMFA solutions [$c_M = 10^{-3}$ mol dm$^{-3}$ for **1**–**7**; $c_M = 10^{-2}$ mol dm$^{-3}$ for **8**–**9**].

in the interval of 111.1–148.6 S cm$^2$ mol$^{-1}$. On the other hand, the values obtained for complexes **7**–**9** clearly show on the fact that they are non-electrolytes (see Table 2). Characteristic IR bands and their assignment are given in Table 2.

### *3.2. IR spectral studies*

For all complexes **1**–**9**, the bands belonging to $\nu$(C···S) and $\nu$(C···N) vibrations were observed at 983–999 cm$^{-1}$, and 1493–1542 cm$^{-1}$, respectively [28,29]. These values clearly characterize the dithiocarbamate moiety. Owing to the fact that intensive bands pertaining to $\nu$(C···S) are not splitted into two components, we can conclude that dithiocarbamate anion is coordinated to nickel in a bidentate fashion. The presence of $ClO_4^-$ in complexes **1**–**3**, **5** and **6**, as well as its ionic nature, can be supported by bands at 1084–1096 cm$^{-1}$ ($\nu_3$) and 622–626 cm$^{-1}$($\nu_4$) [30]. The peak recorded at 2083 cm$^{-1}$ in the spectrum of **4** may be assigned to an asymmetric stretching vibration of an ionic bonded NCS$^-$ anion [31]. The conclusions following from the interpretation of IR spectral data of [Ni(BzMetdtc)$_2$(cyclam)] (**7**) and [Ni(Bz$_2$dtc)$_2$(cyclam)] (**8**) are not unambiguous and at this point, and unfortunately, we cannot make decision if the bidentate manner of coordination of dithiocarbamate would be possible in the case of the discussed complexes. Generally, we may assume the tetradentate coordination of cyclam and the bidentate coordination of each of two dithiocarbamate ligands, and thus, to accept the non-ionic nature of the complexes as determined by conductivity measurements. It would point out that the coordination number for nickel would be eight, and evidently, this is not possible in the case of the ligand's combination used. However, the manner of ligand coordinations in **7** and **8** has been resolved by means of single crystal X-ray analysis and will be explained and discussed in greater details in the Section 3.3.

### 3.3. X-ray structures of [Ni(Bzppzdtc)(phen)$_2$]ClO$_4$ · CHCl$_3$ (3) and [Ni(Bz$_2$dtc)$_2$(cyclam)] (8)

The molecular structure of complex **3** and **8** is depicted in Figs. 1 and 2, respectively. Selected bond lengths and angles are given in Table 4. The molecular structure of [Ni(Bzppzdtc)(phen)$_2$]ClO$_4$ · CHCl$_3$ (**3**) consists of the [Ni(Bzppzdtc)(phen)$_2$]$^+$ cation, perchlorate anion, and CHCl$_3$ as a solvent molecule. The nickel(II) ion is six-coordinated by four nitrogen atoms from two phen ligands and two sulphur atoms from 4-benzylpiperazinedithiocarbamate anion in a distorted octahedral geometry. The [Ni(Bzppzdtc)(phen)$_2$]$^+$ cation contains three different rings, i.e. the phen ligand containing N1 and N2 atoms (ring 1), phen ligand containing N3 and N4 atoms (ring 2) and a part of dithiocarbamate moiety together with the nickel atom involving a NiS$_2$C moiety (ring 3). All three rings are nearly planar with maximal deviation being 0.099(5) Å for C(8), 0.054(4) Å for C(20) and 0.074(4) Å for C(25) in rings 1–3, respectively [24]. The dihedral angle between rings 1 and 2, 1 and 3, and 2 and 3 are equal to 81.88(4)°, 88.65(4)°, and 86.02(4)°, respectively. The delocalization of π-electron density over the S$_2$CN moiety, as typical for a bidentate coordination of any dithiocarbamate anion to a transition metal, may be evident from the C–N and C–S bond length values (see Table 4). For comparison, mean values for C–N, C=S and C–S bonds, as found in Cambridge Structural Database (CSD Version 5.28), are 1.331 Å (valid for S$_2$CNR$_2$ moiety), 1.661 Å (valid for S$_2$CNR$_2$ moiety), and 1.753 Å (valid for R–S–R), respectively [6]. On the other hand, the C–S bond lengths in **3** and **8** are comparable to those as determined for bidentate coordinated dithiocarbamate moieties in case of Ni-complexes (the mean value in delocalized C–S bonds is 1.713 Å) [6]. The ionic nature of ClO$_4^-$ in **3** can be seen from the Ni···Cl separation which is 6.5912(13) Å.

The structure of **8** consists of a centrosymmetric Ni$_{1/2}$(Bz$_2$dtc)(cyclam)$_{1/2}$ moiety which is connected with its second part by means of inversion centre [symmetry code: $^a$ $-x, -y+1, -z+1$]. Thus, the Ni1 atom and some atoms of cyclam adopt non-unit occupancy factors. The crystallographically independent part of the complex molecule is connected with its second centrosymmetric part through partially disordered cyclam ligand. The separation of Ni1···Ni1a is 2.3962(16) Å. The presence of the above-mentioned symmetry operation together with the disorder causes that each of the two parts of the nickel atom is six coordinated by four N atoms from cyclam and two S atoms from a bidentate coordinated dithiocarbamate ligand. Moreover, it also explains why may be coordinated the dithiocarbamate ligand to nickel via two S atoms. It also clearly supports conclusions following from IR data. Similarly as in **3**, a significant delocalization of π-electron density over the S$_2$CN moiety in **8**, as typical for a bidentate coordination of any dithiocarbamate anion to a transition metal, may be evident from the C–N and C–S bond length values (see Table 4).

In conclusion of this section, it is necessary to emphasize that the discussed structures represent the first examples of structurally characterized octahedral Ni-dithiocarbamate complexes bearing a combination of the ligands used.

### 3.4. TG and DTA studies

Thermal stability studies were performed for complexes **4**, **7**, **8** and **9**. The remaining compounds, i.e. those containing perchlorate anions, were not studied for safety reasons.

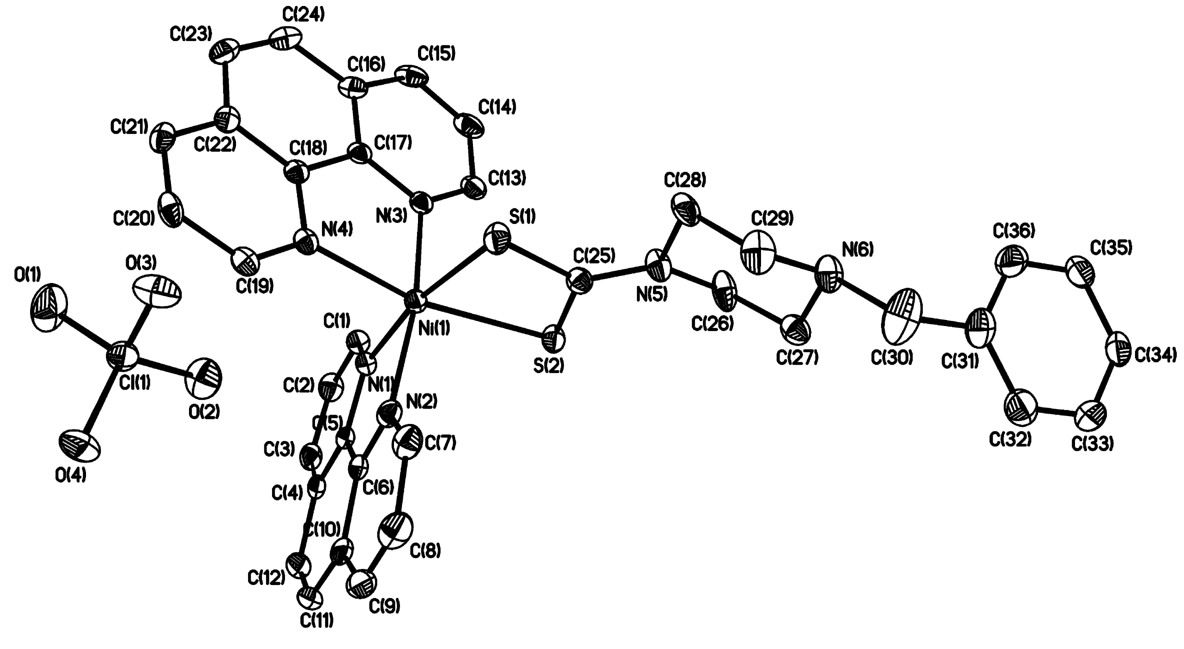

Fig. 1. The molecular structure of [Ni(Bzppzdtc)(phen)$_2$]ClO$_4$ · CHCl$_3$ (**3**) with the atom labelling scheme. Thermal ellipsoids are drawn at the 40% probability level. H-atoms and CHCl$_3$ molecule have been omitted for clarity.

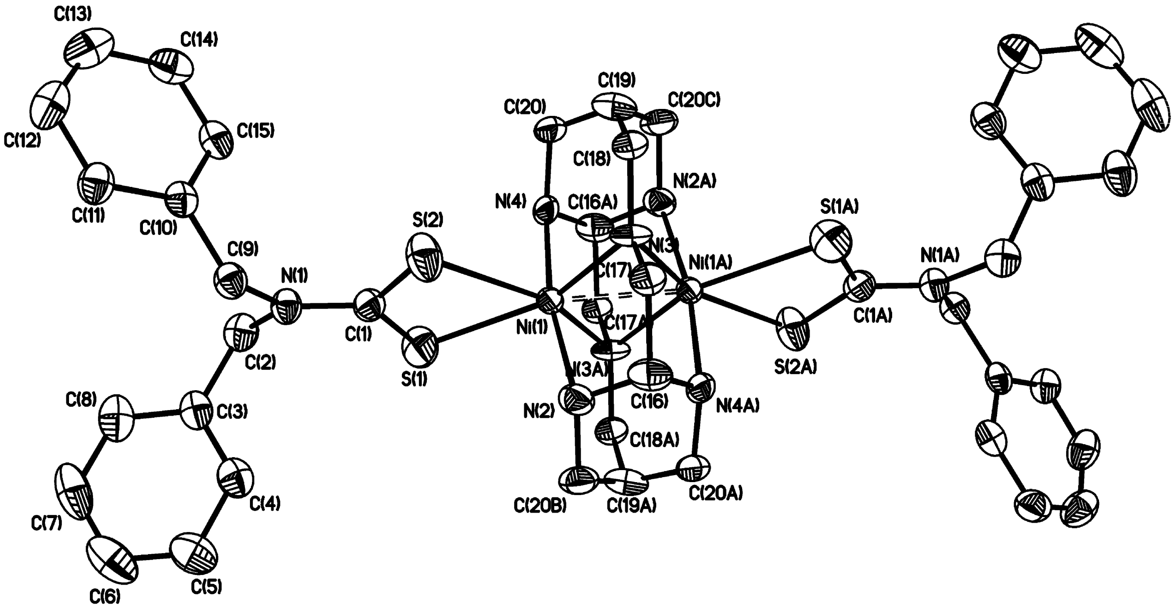

Fig. 2. The molecular structure of [Ni($Bz_2dtc$)$_2$(cyclam)] (**8**) with the atom labelling scheme, showing partially disordered cyclam ligand. Thermal ellipsoids are drawn at the 40% probability level. H-atoms and some of disordered cyclam atoms have been omitted for clarity.

Table 4
Selected bond lengths (Å) and angles (°) for [Ni(Bzppzdtc)(phen)$_2$]$ClO_4 \cdot CHCl_3$ (**3**) and [Ni($Bz_2dtc$)$_2$(cyclam)] (**8**)

| **3** | | | | **8** | | | |
|---|---|---|---|---|---|---|---|
| Ni(1)–N(1) | 2.096(3) | N(1)–Ni(1)–N(2) | 79.29(12) | Ni(1)–N(2) | 2.133(9) | N(3)–Ni(1)–N(4) | 89.3(5) |
| Ni(1)–N(2) | 2.099(3) | N(3)–Ni(1)–N(4) | 79.53(12) | Ni(1)–N(2a) | 2.17(3) | N(3)–Ni(1)–N(2) | 84.2(5) |
| Ni(1)–N(3) | 2.072(3) | S(1)–Ni(1)–S(2) | 73.85(3) | Ni(1)–N(3) | 2.022(12) | N(4)–Ni(1)–N(2) | 170.5(3) |
| Ni(1)–N(4) | 2.099(3) | N(3)–Ni(1)–N(2) | 168.69(10) | Ni(1)–N(3a) | 1.99(2) | S(2)–Ni(1)–S(1) | 69.22(4) |
| Ni(1)–S(1) | 2.4020(11) | N(1)–Ni(1)–S(1) | 170.75(7) | Ni(1)–N(4) | 2.085(9) | S(2)–C(1)–S(1) | 119.0(2) |
| Ni(1)–S(2) | 2.4438(9) | N(4)–Ni(1)–S(2) | 165.63(7) | Ni(1)–N(4a) | 2.13(2) | C(1)–S(1)–Ni(1) | 85.66(13) |
| S(1)–C(25) | 1.719(3) | C(25)–S(1)–Ni(1) | 85.53(11) | Ni(1)–S(1) | 2.5958(15) | C(1)–S(2)–Ni(1) | 86.08(13) |
| S(2)–C(25) | 1.713(4) | C(25)–S(2)–Ni(1) | 84.34(11) | Ni(1)–S(2) | 2.5898(13) | | |
| N(5)–C(25) | 1.334(5) | S(1)–C(25)–S(2) | 116.08(18) | S(1)–C(1) | 1.715(4) | | |
| | | | | S(2)–C(1) | 1.703(4) | | |
| | | | | N(1)–C(1) | 1.344(4) | | |

Generally, we can note that the studied complexes are not comparatively thermally stable. They start to decompose within a relatively broad temperature interval of 134–193 °C. In the case of complexes **4**, **7** and **8**, the decays proceed without formation of thermally stable intermediates in several steps and are not finished even at 1050 °C. The decompositions are accompanied by several *exo*-effects on DTA curves in the case of the discussed complexes. The dominant *exo*-effects were observed at *ca.* 480 °C and it may be probably connected with the decomposition of the organic part of the complex. As for the thermal decay of **9**, the situation is a little bit different. That is why we will discuss it in greater detail. The complex **9** starts to decompose at 190 °C and the beginning of the decay is accompanied by significant decrease in the sample weight (*ca.* 56%). At the first stage of the decomposition, three small *endo*-effects can be seen on the DTA curve with the minimum at 236, 267, and 350 °C, respectively (see Fig. 3). The *endo*-effect with the maximum at 236 °C may be related to melting of the sample which was determined using melting point apparatus to be 234 °C. Next thermal decay proceeds in two waves and is finished at 705 °C. A sharp *exo*-effect with the maximum at 476 °C is clearly seen on the DTA curve, and is probably connected with the burning of the organic part of the molecule. Then, a plateau exists on the TG curve between 706 and 1050 °C. It has been found that the end-product of the thermal degradation is NiO ($\Delta m$ found/calcd., 89.2/91.7%). The product was identified using the Bede ZDS program package [32] and PDF-2 database [33] as NiO (PDF-2 card number: 47–1049).

### 3.5. The catalytic study

For representative complexes **2**, **3**, **6** and **7**, their influence on graphite oxidation was studied. In quest to evaluate obtained results objectively, we also measured the oxidation of pure graphite (gr) and considered an impact of pure acetone (sample 0), as a solvent used for the preparation of the

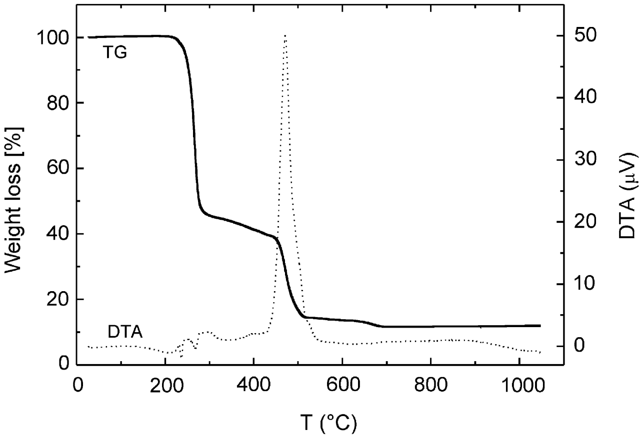

Fig. 3. TG and DTA curves for [Ni($Bz_2dtc$)$_2$(phen)] (**9**).

samples containing the complexes, on the course of the oxidation. A comparison of the oxidation courses of the above-mentioned samples is depicted in the form of their DTG curves in Fig. 4. Characteristic temperatures and kinetic parameters obtained from TG curves are summarized in Tables 5 and 6, respectively. It has been found that acetone application has no significant impact on the graphite oxidation. However, its presence causes only small decrease in temperature of the oxidation (*ca.* 10 °C) together with the decreasing of the activation energy of the process. The presence of the complexes even in applied trace amount (Ni content is about 100 mol ppm) has significant impact on the course of the graphite oxidation, however, this effect is practically independent on the quality of the admixture used, i.e. on the complexes themselves. In the presence of the complexes, the oxidation of graphite starts about 60 °C lower as compared to the sample containing graphite and acetone but the temperature relating to the termination of graphite oxidation is not influenced much. It follows that the width of the temperature interval in which the graphite oxidation with the samples proceeds is about 50 °C greater as compared to pure graphite. It can be seen from shapes of DTG curves that the presence of complexes causes bifurcating of the formerly simple DTG peak, thus graphite enriched by the complexes is oxidized in two steps in comparison of pure graphite.

Table 5
Characteristic temperatures (°C) of graphite, acetone and their mixtures with complexes

| Sample | $T_p$ | $T_m$ | $T_k$ | $T_k - T_p$ |
|---|---|---|---|---|
| Pure graphite (gr) | 775 | 834 | 862 | 87 |
| Pure acetone (0) | 763 | 822 | 854 | 91 |
| **2** | 704 | 806 | 848 | 144 |
| **3** | 706 | 804 | 846 | 140 |
| **6** | 705 | 807 | 848 | 143 |
| **7** | 702 | 807 | 849 | 147 |

$T_p$ – the beginning of oxidation; $T_m$ – oxidation rate maximum; $T_k$ – the end of oxidation.

Table 6
Kinetic parameters of oxidation of graphite, acetone and their mixtures with complexes

| Sample | Step | *n* | $A$ ($s^{-1}$) | $E$ (kJ $mol^{-1}$) | *w* (%) |
|---|---|---|---|---|---|
| Pure graphite (gr) | | 0.7 | $9.50 \times 10^8$ | 241 | |
| Pure acetone (0) | | 0.7 | $1.47 \times 10^8$ | 222 | |
| **2** | I | 1.0 | $5.36 \times 10^5$ | 160 | 53.66 |
| | II | 1.3 | $1.17 \times 10^{17}$ | 400 | 46.34 |
| **3** | I | 0.9 | $1.24 \times 10^5$ | 150 | 58.30 |
| | II | 1.1 | $1.35 \times 10^{14}$ | 341 | 41.70 |
| **6** | I | 1.0 | $6.00 \times 10^5$ | 162 | 60.91 |
| | II | 1.4 | $3.92 \times 10^{20}$ | 474 | 39.09 |
| **7** | I | 1.0 | $2.43 \times 10^5$ | 155 | 63.13 |
| | II | 1.2 | $3.23 \times 10^{17}$ | 412 | 36.87 |

*n* – reaction order; *A* – frequency factor, *E* – activation energy, *w* – mass of sample oxidized.

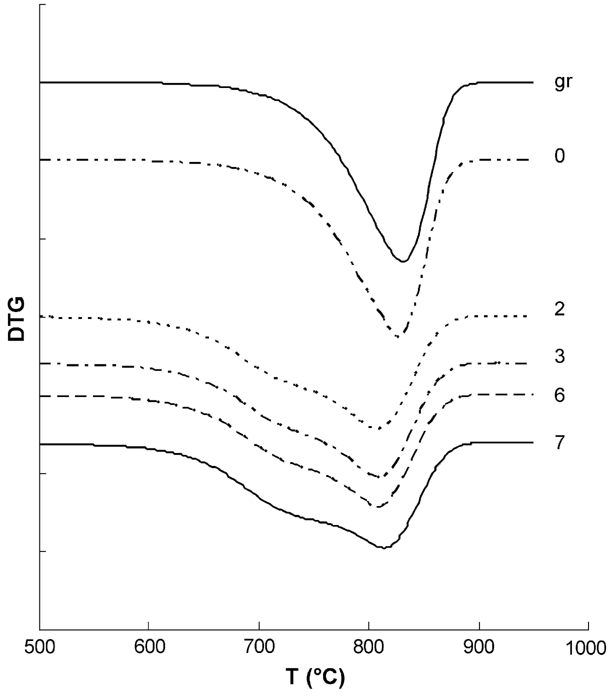

Fig. 4. DTG curves of graphite samples containing complexes **2**, **3**, **6** and, their comparison with DTG curves for pure graphite (gr) and pure acetone (0).

The calculated values of activation energies (*E*) and frequency factors (*A*) show that two observed oxidative steps of the enriched graphite differ significantly. A bigger portion of graphite is oxidized in the first step with activation energy values of 150–160 kJ $mol^{-1}$ and frequency factors in the order of $10^5$–$10^6$ $s^{-1}$. Significantly higher values of both parameters were determined for the second step. The reaction order was determined to be slightly higher for both steps ($n = 1.0$–$1.4$; see Table 6) as compared to free graphite ($n = 0.7$). It shows the fact that the kinetics of pure graphite is determined by its contracting volume ($n = 2/3$ corresponds to phase boundary controlled reaction, i.e. mechanism R3), however, the kinetics of oxidation of graphite enriched by the complexes can be described better by the model of the first-order reaction.

## Acknowledgements

The financial support of this work by The Ministry of Education, Youth and Sports of the Czech Republic (a grant no. MSM6198959218) is gratefully acknowledged. Authors also wish to thank to Mrs. Regina Mencelová for help with the preparation of some complexes, Dr. Zdeněk Šindelář for magnetic susceptibility measurements and Mr. Pavel Štarha for performing of TG/DTA measurements.

## Appendix A. Supplementary material

CCDC 625271 and 652556 contain the supplementary crystallographic data for complexes **3** and **8**, respectively. These data can obtained free of charge via http://www.ccdc.cam.ac.uk/conts/retrieving.html, or from the Cambridge Crystallographic Data Centre, 12 Union Road, Cambridge CB2 1EZ, UK; fax: (+44) 1223-336-033; or e-mail: deposit@ccdc.cam.ac.uk. Supplementary data associated with this article can be found, in the online version, at doi:10.1016/j.poly.2007.09.024.

## References

[1] D. Coucouvanis, J.P. Fackler Jr., Inorg. Chem. 6 (1967) 2047.
[2] R. Dingle, Inorg. Chem. 10 (1971) 1141.
[3] K. Ramalingam, G. Aravamudan, V. Ventachalam, Bull. Chem. Soc. Jpn. 66 (1993) 1554.
[4] R. Pastorek, F. Březina, Z. Šindelář, M. Klečková, Acta Univ. Palacki. Olom. 97 (1990) 19.
[5] R. Pastorek, J. Kameníček, M. Pavlíček, J. Husárek, Z. Šindelář, Z. Žák, Acta Univ. Palacki. Olom. 40 (2001) 57.
[6] F.H. Allen, Acta Crystallogr. Sect. B – Struct. Sci. 58 (2002) 380.
[7] Ng. Szeman, J.W. Ziller, P.J. Farmer, Inorg. Chem. 43 (2004) 8301.
[8] V. Shklover, T. Haibach, B. Bolliger, M. Hochstrasser, M. Erbudak, H.U. Nissen, S.M. Zakeeruddin, M.K. Nazeeruddin, M. Gratzel, J. Solid State Chem. 132 (1997) 60.
[9] S.M. Zakeeruddin, Md.K. Nazeeruddin, R. Humphy-Baker, M. Gratzel, V. Shklover, Inorg. Chem. 37 (1998) 5251.
[10] G.D. Forster, G. Hogarth, J. Chem. Soc., Dalton Trans. (1993) 2539.
[11] T.A. Coffey, G.D. Forster, G. Hogarth, J. Chem. Soc., Dalton Trans. (1995) 2337.
[12] G. Hogarth, I. Richards, Dalton Trans. (2005) 760.
[13] M. Kita, K. Yamanari, Y. Shimura, Bull. Chem. Soc. Jpn. 62 (1989) 23.
[14] S.P. Sovilj, K.B. Babic-Samardzija, Hemijska Industrija (Chem. Ind.) 54 (2000) 534.
[15] R. Vicente, A. Escuer, J. Ribas, A. Dei, X. Solans, T. Calvet, Polyhedron 9 (1990) 1729.
[16] R. Pastorek, J. Kameníček, B. Cvek, V. Slovák, M. Pavlíček, J. Coord. Chem. 59 (2006) 911.
[17] R. Pastorek, J. Kameníček, H. Vrbová, V. Slovák, M. Pavlíček, J. Coord. Chem. 59 (2006) 437.
[18] R. Pastorek, J. Kameníček, B. Cvek, M. Pavlíček, Z. Šindelář, Z. Žák, J. Coord. Chem. 56 (2003) 1123.
[19] R. Přibil, Komplexometrické titrace, SNTL, Praha, 1955, p. 22.
[20] M. Jureček, Organická analýza II, ČSAV, Praha, 1957, p. 140.
[21] V. Slovák, Thermochim. Acta 372 (2001) 175.
[22] G.M. Sheldrick, Acta Crystallogr. A 46 (1990) 467.
[23] G.M. Sheldrick, SHELXL-97, Program for crystal structure refinement, University of Göttingen, Göttingen, Germany, 1997.
[24] K. Brandenburg, H. Putz, DIAMOND (Version 3.1e), Crystal and molecular structure visualization, Crystal Impact GbR, Postfach 1251, Bonn, Germany, 2007.
[25] S.G. Vulfson, Molecular Magnetochemistry, Gordon and Breach Science Publishers, The Netherlands, 1998, p. 354.
[26] A.B.P. Lever, Inorganic Electronic Spectroscopy, second ed., Elsevier, Amsterdam, 1984, p. 534.
[27] W.J. Geary, Coord. Chem. Rev. 7 (1971) 81.
[28] C.A. Tsipis, D.P. Kessissoglou, G.A. Katsoulos, Chim. Chron., New Series 14 (1985) 195.
[29] I.E. Černikova, I.A. Chartonik, D.S. Umrejko, A.B. Kavrikov, V.I. Afanov, Koord. Chim. 15 (1989) 1695.
[30] R.P. Scholer, E.A. Merbach, Inorg. Chim. Acta 15 (1975) 15.
[31] K. Nakamoto, Infrared and Raman Spectra of Inorganic and Coordination Compounds: Part B: Applications in Coordination, Organometallic, and Bioinorganic Chemistry, fifth ed., Wiley, New York, 1997, p. 116.
[32] Bede ZDS Search/Match for Windows, Ver. 4.53, Bede Scientific Instruments Ltd., Durham, United Kingdom, 2000.
[33] PDF-2 Database Sts 1-47, (1997). ICDD, 12 Campus Boulevard, Newtown Square, Pennsylvania 19073-3273, USA.